

A theoretical view of practical problems in interferometry

A. Makhlin, E. Surdutovich, and G. Welke*

Department of Physics and Astronomy, Wayne State University, Detroit MI 48202, USA

Interferometry is discussed in terms of the representation of the source. In particular, scale-invariant 1-d hydrodynamics is revisited, and extended to the case of unequal transverse masses. It is argued that kaon emission occurs over a short time interval. Exact results for models of two- and three-dimensional flow are presented, which exhibit altered scaling laws. Such qualitative trends, together with other observables, are vital if one is to draw conclusions about the source [1].

I. INTRODUCTION

The discovery a quark-gluon plasma will to some extent be linked to the measurement of the geometric size and other macroscopic characteristics of the reaction zone. An important tool in accomplishing this is interferometry. As proposed by Hanbury-Brown and Twiss to measure stellar sizes, and as the GGLP effect in (low energy) nuclear physics, it provides for a straightforward determination of the size of the “hot source.” In high-energy collisions, on the other hand, the correspondence between measured quantities and parameters of the emitting system is less clear [2]. For example, correlations on the same scale as the size of the emitting system make an interferometric study of the correlations inside the matter and a measurement of the external geometry exceedingly difficult [3].

For A-A collisions, even in the simplest scenario of hydrodynamic evolution, the relation between the inclusive one- and two-particle spectra and the parameters of the emitting system does not follow the classical scheme of interferometry [4]. Since no direct inverse solution exists, and the question of *what* is measured by the two-pion correlation function becomes nontrivial. The problem for interferometry is thus to determine the parameters of a judiciously chosen density matrix ρ for the system, by measuring the inclusive cross-sections $dN_1/d\vec{k}$, $dN_2/d\vec{k}_1 d\vec{k}_2, \dots$. Here, we shall restrict ourselves to particle sources that may be described in terms of (semi-) classical one-particle distributions, or even by only a few macroscopic parameters. Practically, current dynamical models produce precisely such sources. However, even with these restrictions, the two-particle spectra are not easily decoded. We therefore suggest in Sect III an illustrative “step-by-step” strategy: Essentially, the data are first confronted with the simplest physically motivated model, and discrepancies are then used show directions for improvement. Ideally, this requires that the model should have an “adequate” (semi-) analytical solution for the correlator, allowing one to obtain the model parameters precisely and directly, without resorting to intermediate fits to the data.

Recent SPS experiments [5,6] have observed m_\perp scaling of longitudinal radii, as well as the y -dependence of the correlator width predicted by boost-invariant 1-d hydrodynamic expansion [7]. This provides a strong reason for taking macroscopic collective behavior (*i.e.*, hydrodynamics) seriously and using interferometry to study it – at least at SPS energies. Here, we shall therefore extend the calculation of Ref. [7] to give the (analytic) solution in the case of unequal transverse momenta, and illustrate why the data support a relatively rapid freeze-out picture for both pions and kaons. We also discuss natural extensions of the model to one that might be more appropriate at the AGS: (1) 1-d Landau hydrodynamics, and (2) some exactly calculable examples with two- and three-dimensional flow. In these cases, the scaling law is altered, and we argue generally that such qualitative trends, together with other observables, are important in establishing an adequate model of the source, and only then the value of its parameters.

Before turning our attention to these matters, however, we discuss a related issue: there is no full consensus on what mathematical formulation is adequate for applications of interferometry. For example, an analysis of polarization effects in photon interference [8] indicates that the languages of locally defined states and Wigner phase-space distributions lead to different answers; there is a practical need to resolve such controversies. We shall therefore begin in Sec. II by briefly formulating the problem of interferometry for an expanding source at the *operator* level. This emphasizes the quantum nature of the problem, and allows us to solve (correctly) the basic problem of one- and two-particle propagation without having to address the unknown nature of the source. With these expressions in hand, we discuss three examples of source input.

*Submitted by G. Welke for Proceedings, HIPAGS '96 Workshop, August 22–24, 1996, Wayne State University, Detroit, Michigan

II. PRELIMINARIES

Let $|\text{in}\rangle$ be any one of the initial states of a system emitting a pion field $\hat{\varphi}(x)$ at time t_c . This field is detected later by an analyzer, tuned to the measurement of the momentum of the free pion; its eigenfunctions are thus plane waves $f_{\vec{k}}(x)$ with $x^0 > t_c$, and the corresponding annihilation operators $\hat{A}_{\vec{k}}$ for momentum \vec{k} in the final state are given by

$$\hat{A}_{\vec{k}} = \int d^3x f_{\vec{k}}^*(x) i \overset{\leftrightarrow}{\partial}_x \hat{\varphi}(x) \quad , \quad (2.1)$$

where $(a \overset{\leftrightarrow}{\partial}_x b) \equiv a(\partial_x^0 b) - (\partial_x^0 a)b$. The operator $\hat{A}_{\vec{k}}$ describes the effect of a detector far from the point of emission, so, by definition, the pion is detected on-mass-shell. The inclusive amplitudes to find one pion with momentum \vec{k} , or two with momenta \vec{k}_1, \vec{k}_2 in the final state are $\langle X | \hat{A}_{\vec{k}} \hat{S} | \text{in} \rangle$ and $\langle X | \hat{A}_{\vec{k}_2} \hat{A}_{\vec{k}_1} \hat{S} | \text{in} \rangle$, respectively. Here, \hat{S} is the evolution operator after freeze-out, and the $|X\rangle$ form a complete set of all possible secondaries. One obtains the one- and two-particle inclusive spectra by summing the squared modulus of these amplitudes over all (undetected) states $|X\rangle$, and averaging over the initial ensemble ρ .

An analyzer tuned to \vec{k} for singles, or \vec{k}_1, \vec{k}_2 for pairs, is represented by the operators

$$\hat{N}(\vec{k}) = \hat{A}_{\vec{k}}^\dagger \hat{A}_{\vec{k}} \quad , \quad \text{and} \quad \hat{N}(\vec{k}_1, \vec{k}_2) = \hat{A}_{\vec{k}_1}^\dagger \hat{A}_{\vec{k}_2}^\dagger \hat{A}_{\vec{k}_2} \hat{A}_{\vec{k}_1} = \hat{N}(\vec{k}_1)(\hat{N}(\vec{k}_2) - \delta(\vec{k}_1 - \vec{k}_2)) \quad , \quad (2.2)$$

respectively. In the simplest description, the pion field $\hat{\varphi}(x)$ reaches the detector after free propagation

$$\hat{\varphi}(x) = \int d\Sigma_\mu(y) G_{\text{ret}}(x-y) \overset{\leftrightarrow}{\partial}_y^\mu \hat{\varphi}(y) \quad , \quad (2.3)$$

where the field $\hat{\varphi}(y)$ and the space of states in which the density matrix acts are defined on the freeze-out hypersurface Σ_c . The pion Fock operator (2.1) may now be expressed in terms of the initial fields, and simplified using the explicit form of the free pion propagators:

$$\hat{S}^\dagger \hat{A}_{\vec{k}} \hat{S} = \theta(x^0 - y^0) \int d\Sigma_\mu(y) f_{\vec{k}}^*(y) i \overset{\leftrightarrow}{\partial}_y^\mu \hat{\varphi}(y) \quad . \quad (2.4)$$

Clearly, the analyzers perform an on-shell Fourier expansion of the initial data. Collecting these results, we may rewrite the number operators for single and pairs as

$$\hat{N}(\vec{k}) = \theta(x^0 - y^0) \int d\Sigma_\mu(y_1) d\Sigma_\nu(y_2) \left[f_{\vec{k}}^*(y_1) i \overset{\leftrightarrow}{\partial}_{y_1}^\mu \hat{\varphi}^\dagger(y_1) \right] \left[\hat{\varphi}(y_2) i \overset{\leftrightarrow}{\partial}_{y_2}^\nu f_{\vec{k}}^*(y_2) \right] \quad (2.5)$$

$$\begin{aligned} \hat{N}(\vec{k}_1, \vec{k}_2) &= \theta(x^0 - y^0) \int d\Sigma_\mu(y_1) d\Sigma_\nu(y_3) d\Sigma_\rho(y_4) d\Sigma_\lambda(y_2) \\ &\times \left[f_{\vec{k}_1}^*(y_1) f_{\vec{k}_2}^*(y_3) \overset{\leftrightarrow}{\partial}_{y_1}^\mu \overset{\leftrightarrow}{\partial}_{y_3}^\nu \hat{\varphi}^\dagger(y_1) \hat{\varphi}^\dagger(y_3) \right] \left[\hat{\varphi}(y_4) \hat{\varphi}(y_2) \overset{\leftrightarrow}{\partial}_{y_4}^\rho \overset{\leftrightarrow}{\partial}_{y_2}^\lambda f_{\vec{k}_2}^*(y_4) f_{\vec{k}_1}^*(y_2) \right] \quad , \quad (2.6) \end{aligned}$$

respectively. The field operator products in these equations are now to be averaged over the density matrix of initial states. The interferometry problem requires that the basis the final *quantum* states of the preceding stage of evolution should be described explicitly. We give three examples:

1. Emission from two one-dimensional cavities: We have two sets of the eigenstates

$$\begin{aligned} \phi_{p,N}(y) &= (2a)^{-1/2} (2p_0)^{-1/2} e^{-ip \cdot y} \quad , \quad \text{for } L_N - a \leq y \leq L_N + a \quad , \quad \text{where } L_N = \pm L \\ &= 0 \quad , \quad \text{otherwise.} \end{aligned} \quad (2.7)$$

The field decomposition $\hat{\varphi}(y) = \sum_{p,N} \hat{a}_{p,N} \phi_{p,N}(y)$ acquires an additional index enumerating the cavities, and states belonging to different cavities are independent: $[\hat{a}_{p,N}, \hat{a}_{p',N'}^\dagger] = \delta_{pp'} \delta_{NN'}$. From Eq. (2.5), the one-particle distribution for when the walls are removed at $y_0 = 0$ is obtained as

$$\langle \hat{N}(k) \rangle = \sum_N \sum_p n(p, N) \frac{(\omega_k + \omega_p)^2}{4\omega_k \omega_p} \frac{\sin^2(p-k)a}{\pi a(p-k)^2} \quad , \quad (2.8)$$

where $n(p, N) = \langle \hat{a}_{p,N}^\dagger \hat{a}_{p,N} \rangle$ is the boson occupation number in cavity N .

For the two-particle spectrum there is interference between four amplitudes: two when each particle is emitted from a different cavity, and two more when both particles originate from the same cavity. For the statistical average of Eq. (2.6) we choose

$$\langle \hat{a}_1^\dagger \hat{a}_3^\dagger \hat{a}_4 \hat{a}_2 \rangle = n(1)n(3) \left[\delta_{p_1 p_2} \delta_{N_1 N_2} \delta_{p_3 p_4} \delta_{N_3 N_4} + \delta_{p_1 p_4} \delta_{N_1 N_4} \delta_{p_3 p_2} \delta_{N_3 N_2} \right], \quad (2.9)$$

where we have introduced the notation $i \equiv (p_i, N_i)$. Then

$$\begin{aligned} \langle \hat{N}(k_1, k_2) \rangle &= \langle \hat{N}(k_1) \rangle \langle \hat{N}(k_2) \rangle + \sum_{1,3} \frac{(\omega_{k_1} + \omega_{p_1})(\omega_{k_1} + \omega_{p_3})(\omega_{k_2} + \omega_{p_1})(\omega_{k_2} + \omega_{p_3})}{4\pi^2 4a^2 4\omega_{k_1} \omega_{k_2} \omega_{p_1} \omega_{p_3}} \times \\ n(1)n(3) &\frac{\sin(p_1 - k_1)a}{(p_1 - k_1)} \frac{\sin(p_1 - k_2)a}{(p_1 - k_2)} \frac{\sin(p_3 - k_1)a}{(p_3 - k_1)} \frac{\sin(p_3 - k_2)a}{(p_3 - k_2)} e^{-i(L_1 - L_3)(k_1 - k_2)}, \end{aligned} \quad (2.10)$$

where $L_j = L(N_j) = \pm L$, and momentum p_j originates from the cavity N_j . The two terms in the sum with $N_1 \neq N_3$ lead to the usual interference term, with $\Delta k \sim 1/(2L)$. The average of the product of Fock operators (2.9), *i.e.*, correlations in the emitting system, depends only on “internal” variables which identify the stationary states in the cavities before they are opened. On the other hand, the sin-functions serve as the projectors of these states onto the states of free propagation in which the particles are detected, and require additional physical input. First, detector resolution should not allow one to determine which cavity the particle originated from, *i.e.*, we do not have $|k_1 - k_2| L \gg 1$. This condition corresponds to the Rayleigh criterium: we are not able to construct an “optical” image of source. Secondly, in most physical situations $L \gg a$, so that $|k_1 - k_2| a \ll 1$. This inequality removes the momentum integral in Eq. (2.8), so that a measurement of the one-particle spectrum does not allow for a determination of the cavity size.

2. Emission from many cavities and hydrodynamics: To generalize the two-cavity model to the freeze-out of an extended hydrodynamic system, we consider a continuous set of decaying thermal cells, defined on a freeze-out surface $T(x) = T_c$ and Doppler shifted to account for cell motion [7]. As in the previous example, the initial quantum states in one cell are assumed to commute with states in a different cell. This additional information implies the existence of two length scales, and allows us to use a quasi-classical picture. Within a cell, the system is governed by the short-range dynamics conveniently described in momentum language and if the interactions are switched off, the particles begin to propagate freely with the frozen momentum distribution defined *within the cell*. To the lowest approximation of the dynamical interactions and in agreement with the freeze-out concept, these particles are on-mass-shell. In terms of an auxiliary “emission function” $J(k_1, k_2)$,

$$J(k_1, k_2) \equiv \int_{\Sigma_c} d\Sigma_\mu(x) \frac{k_1^\mu + k_2^\mu}{2} n(k_1 \cdot u(x)) e^{-i(k_1 - k_2)x}, \quad (2.11)$$

one obtains for the one- and two-particle spectra [7]:

$$k^0 \frac{dN_1}{d\vec{k}} = J(k, k), \quad \text{and} \quad k_1^0 k_2^0 \frac{dN_2}{d\vec{k}_1 d\vec{k}_2} = J(k_1, k_1) J(k_2, k_2) + \text{Re} \left[J(k_1, k_2) J(k_2, k_1) \right], \quad (2.12)$$

respectively. The latter equation is explicitly symmetric in x_1 and x_2 , as well as in k_1 and k_2 . It reveals interference of the two amplitudes for the two-pion state (consisting of the two on-mass-shell pions with quantum numbers \vec{k}_1 and \vec{k}_2) to be emitted by the two sources. These sources are located at points x_1 and x_2 and have true thermal distributions, $n(k_i \cdot u(x_i))$, with on-shell particles.

3. Wigner formalism: Simulations of heavy ion collisions typically produce a final state in terms of Wigner distributions, so it is of practical value to examine the two-particle spectrum in terms of them. Instead of Eq. (2.9), we may express the independence of the dynamical processes in the emitting system via

$$\langle \hat{\varphi}^\dagger(x) \hat{\varphi}^\dagger(x') \hat{\varphi}(y) \hat{\varphi}(y') \rangle = \langle \hat{\varphi}^\dagger(x) \hat{\varphi}(y) \rangle \langle \hat{\varphi}^\dagger(x') \hat{\varphi}(y') \rangle + \langle \hat{\varphi}^\dagger(x) \hat{\varphi}(y') \rangle \langle \hat{\varphi}^\dagger(x') \hat{\varphi}(y) \rangle \quad (2.13)$$

which implies that the distance $z = x - y$ between the points in one correlator does not exceed a correlation length a_{cor} which, in turn, is much less than the full size L of the system. In the first term, for example, $x, y \sim R_1$, $x - y < a_{cor}$ and $x', y' \sim R_2$, $x' - y' < a_{cor}$, while $R_1 - R_2 \gg a_{cor}$. Under these conditions, it is possible to think of the coordinates

R_j as labels of domains of non-vanishing correlation, while the Fourier transform over \vec{z} yields the local spectrum. Thus, changing variables¹ $x = R + z/2$, $y = R - z/2$, and introducing the Wigner function \mathcal{N}

$$\langle \hat{\varphi}^\dagger(R + \frac{z}{2}) \hat{\varphi}(R - \frac{z}{2}) \rangle = \int d^3s \mathcal{N}(\vec{R}, \vec{s}) e^{i\vec{s}\cdot\vec{z}} \quad , \quad (2.14)$$

Eqs. (2.6), (2.13), and (2.14) yield

$$\begin{aligned} \langle \hat{N}(k_1, k_2) \rangle &= \int dR_1 dz_1 ds_1 \mathcal{N}(\vec{R}_1, \vec{s}_1) e^{i(s_1 - k_1)z_1} \int dR_2 dz_2 ds_2 \mathcal{N}(\vec{R}_2, \vec{s}_2) e^{i(s_2 - k_2)z_2} + \\ &\int dR_1 dR_2 dz_1 dz_2 ds_1 ds_2 \mathcal{N}(\vec{R}_1, \vec{s}_1) \mathcal{N}(\vec{R}_2, \vec{s}_2) e^{-i(k_1 - k_2)(R_1 - R_2)} e^{-i(\frac{k_1 + k_2}{2} - s_1)z_1 - i(\frac{k_1 + k_2}{2} - s_2)z_2} \quad . \end{aligned} \quad (2.15)$$

If the range of integration a_{cor} (which, strictly speaking, depends on R) for the z -variable is sufficiently large compared to $1/k_1$, $1/k_2$, the integrals over z_1 and z_2 approximate to delta-functions, and the common expression for the correlator C_2 in terms of functions $\mathcal{N}((k_1 + k_2)/2, \vec{R})$ results [4]. Physically, however, since the $\hat{\varphi}(x)$ are free, there are no states with $s^2 \neq m^2$. We thus face the problem of understanding the origin of a thermal distribution of off-shell pions, instantly frozen, and detected later in physical on-shell states.² The variables of integration do not correctly establish the correspondence between initial and final states. Moreover, the replacement $\mathcal{N}((k_1 + k_2)/2, \vec{R})$ undermines the concept of independent emission of the two sources – a necessary condition for interference. Each source “knows” about the momenta of both pions, and one may reasonably suspect that emission from spatially separated volumes is not independent.

III. INTERFEROMETRY AND SOURCE MODELS

1. One-dimensional flow: We revisit interferometry for scale invariant 1-d hydrodynamic motion; evidence for such sources at SPS [5,6] comes from agreement with the theoretically predicted [7] m_t - and y -dependence of the “visible longitudinal size:”

$$R_L = \frac{\tau}{\cosh y} \sqrt{\frac{T_c}{m_t}} \quad . \quad (3.1)$$

where y is the pair mid-rapidity, and $m_t^2 = m^2 + p_t^2$. Physically, the correlator measures the effective size of the fluid slice which forms the observable spectrum at a given rapidity. The larger the transverse momentum of a particle in the fluid, the more that particle is frozen into collective longitudinal motion: the subset of particles with high p_\perp will have a very narrow distribution over k_\parallel .

The dependence (3.1) was derived for the case of equal transverse momenta. This condition is impractical and not the way the data were taken, so we extend the calculations to the case of unequal transverse masses. The parameters of the model are the critical temperature, T_c ($\sim m_\pi$), and the space-like freeze-out hypersurface, $t^2 - x_\parallel^2 = \tau^2 = \text{const}$. We assume a Gaussian transverse distribution $\exp(-r_\perp^2/R_\perp^2)$ of hot matter in a pipe with effective area $S_\perp = \pi R_\perp^2$. The particles are described by their momenta $k_i^\mu = (k_i^0, k_i^\parallel, \vec{p}_i) \equiv (m_i \cosh \theta_i, m_i \sinh \theta_i, \vec{p}_i)$, where \vec{p}_i is the transverse momentum, θ_i the particle rapidity in the beam direction, and $m_i^2 = m_\pi^2 + \vec{p}_i^2$ is the transverse mass. Further, let $2\alpha = \theta_1 - \theta_2$, $2\theta = \theta_1 + \theta_2$ and $\vec{q}_\perp = \vec{p}_1 - \vec{p}_2$. Approximating the one-particle distribution by a Boltzmann form, the saddle point method yields from Eq. (2.11) (see Ref. [1]):

$$\frac{dN}{d\theta_1 d\vec{p}_1} \approx \tau S_\perp m_1 \sqrt{\frac{2\pi T_c}{m_1}} e^{-m_1/T_c} \quad , \quad (3.2)$$

and

¹A formal change of variables can already be made at the operator level, Eq. (2.6), but the calculation of the two-particle spectrum then becomes ambiguous [1]. ²The problem is even more acute for photon emission: unphysical longitudinally polarized states are introduced [1,8].

$$\begin{aligned}
C_2(k_1, k_2) - 1 &= \frac{dN_2}{d\theta_1 d\bar{p}_1 d\theta_2 d\bar{p}_2} / \left[\frac{dN_1}{d\theta_1 d\bar{p}_1} \frac{dN_1}{d\theta_2 d\bar{p}_2} \right] - 1 \\
&\approx \frac{1}{4} f(|\vec{q}_\perp| R_\perp) \frac{g(z) g(1/z)}{[h(z) h(1/z)]^{3/2}} \exp \left\{ -\frac{\mu}{T_c} \left[h(z) \cos \frac{H(z)}{2} + h\left(\frac{1}{z}\right) \cos \frac{H(1/z)}{2} - z - \frac{1}{z} \right] \right\} \\
&\times \cos \left\{ \frac{\mu}{T_c} \left[h(z) \sin \frac{H(z)}{2} + h\left(\frac{1}{z}\right) \sin \frac{H(1/z)}{2} \right] + \frac{3}{4} \left[H(z) + H\left(\frac{1}{z}\right) \right] + G(z) + G\left(\frac{1}{z}\right) \right\},
\end{aligned} \tag{3.3}$$

where $\mu = (m_1 m_2)^{1/2}$ and $z = (m_1/m_2)^{1/2}$, and we have introduced the functions

$$\begin{aligned}
h(z) &\equiv \left\{ \left[z^2 - F^2 \left(z - \frac{1}{z} \right)^2 + 4F^2 \sinh^2 \alpha \right]^2 + 4F^2 (z^2 - \cosh 2\alpha)^2 \right\}^{1/4}; \\
g(z) &\equiv \left[(z^2 + \cosh 2\alpha)^2 + F^2 \left(z^2 - \frac{1}{z^2} \right)^2 \right]^{1/2}; \quad f(|\vec{q}_\perp| R_\perp) = e^{-\vec{q}_\perp^2 R_\perp^2 / 2}
\end{aligned} \tag{3.4}$$

$$\tan H(z) = \frac{2F(\cosh 2\alpha - z^2)}{z^2 - F^2 \left(z - \frac{1}{z} \right)^2 + 4F^2 \sinh^2 \alpha}; \quad \tan G(z) = \frac{F(z^2 - 1/z^2)}{z^2 + \cosh 2\alpha}. \tag{3.5}$$

with $F = \tau T_c$. Equation (3.3) is free of the limitation $m_1 = m_2$, and should be used directly to fit the model parameters, T_c and τ , without an intermediate Gaussian, and at various rapidities. The T_c may then in turn be confronted with the slope of the one-particle spectrum. If, for instance, we find a dependence $\tau(y)$ then it is natural to consider the effect of a finite initial size via the 1-d Landau model as a next step. The visible size will be given by Eq. (3.1), with $\tau \rightarrow \tau(y)$ [7]. Now, the relevant parameters of the model are the initial size and temperature, and the shape of the freeze-out surface. The general idea is that since there is no unique prescription to decode the interferometric data, the most effective approach is a “step-by-step” strategy – the complexity of the models used to fit the data should increase gradually in directions which are suggested by a thorough analysis of the simpler model.

It has been conjectured [9] that kaons may escape from the source earlier and over a longer period of time than pions. Such a “dynamical” decoupling will influence the interferometric data. Suppose first that we have a sharp and common freeze-out of all particles; taking $T_c = 130$ MeV and $\tau = 30$ fm, we obtain the curves marked “s” in Fig. 1. As expected, we find that $\gamma \equiv a_{eff} m_\perp^{1/2}$ is independent of m_\perp , and $\gamma_\pi = \gamma_K$. Suppose on the other hand that the kaons decouple dynamically from the pion fluid over some interval from τ_0 to τ ; if $\tau_0 = 7$ fm ($\tau T^3 = \text{const}$ then implies $T_0 = 180$ MeV), and assuming for simplicity an unweighted average of emission function (2.11), $\langle J(\tau) \rangle_\tau$, we obtain the curves marked “g.” Clearly, m_\perp -scaling is violated for this type of emission. NA44 data [6] gives no indication of such scaling violation, suggesting that the kaon fluid remains coupled to the pions right until their common (sharp) freeze-out. A systematic and parallel study of pion and kaon interferometric source sizes as a function of m_\perp will provide a sensitive test for the temporal interval of freeze-out in hadronic matter at RHIC.

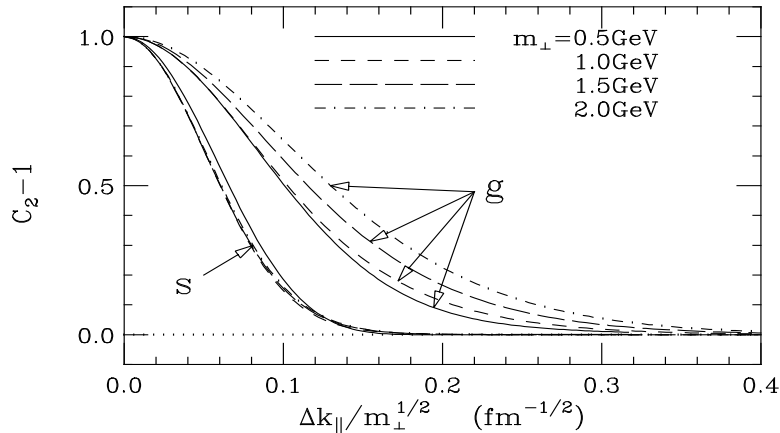


FIG. 1. The correlation function C_2 , as a function of the rescaled longitudinal momentum difference.

The dependence (3.1) may well apply at the SPS energies, since most of the matter will cool and reach the freeze-out stage due to the fast longitudinal expansion rather than the much slower transverse expansion, but at the AGS it is well known that transverse flow plays an important role. We illustrate the effects one might encounter by way of two unphysical, but exactly calculable examples:

2. Scale-invariant 2-d flow and the explosion of a long filament: To find a possible signature of transverse flow, consider the extreme case of a transversely expanding filament of length $L \gg R_\perp$. A convenient parameterization of the coordinates is $x^\mu = (\tau \cosh \beta, \tau \sinh \beta \cos \psi, \tau \sinh \beta \sin \psi, z)$, where β is the radial rapidity of the fluid cell. The temperature and velocity field may be written as $\tau^2 T_c^3 = \text{const}$, and $u^\mu = (\cosh \beta, \sinh \beta \cos \psi, \sinh \beta \sin \psi, 0)$, while $d\Sigma^\mu = u^\mu \tau^2 \sinh \beta dz d\beta d\psi$. The emission function $J(k_1, k_2)$ may be calculated exactly for $m_{z1} = m_{z2}$, where $m_z = \sqrt{p_z^2 + m^2}$ is the longitudinal mass. We obtain

$$k^0 \frac{dN_1}{d\vec{k}} = J(k, k) = 2\pi L \tau^2 T_c \frac{e^{-m_z/T_c}}{(m_z/T_c)} \left[\frac{m_z}{T_c} - 1 \right] , \quad (3.6)$$

$$C_2(k_1, k_2) - 1 = \text{Re} \frac{e^{-2m_z(H-1)/T_c}}{H^6} \left[\frac{m_z H/T_c + 1}{m_z/T_c + 1} \right]^2 \left[1 + \frac{Q^2}{8m_z^2} \right]^2 , \quad (3.7)$$

$$\text{where } Q^2 = -(k_1 - k_2)^2, \quad H = \left[1 + T_c^2 \tau^2 \frac{Q^2}{m_z^2} - i \frac{T_c \tau Q^2}{2m_z^2} \right]^{1/2} . \quad (3.8)$$

Similar to the case of 1-d boost invariant flow, we obtain a plateau for cylindrical boost invariant expansion, but now in the radial rapidity distribution. The dependence of the spectral density on m_z is noteworthy: the localization of the spectrum due to radial flow is more pronounced for greater m_z . Particles with $m_z/T_c \gg 1$ spend almost all their thermal energy for the longitudinal motion and thus are strongly frozen into collective radial flow. For this reason we may expect the width of the correlator in the transverse direction to be defined by m_z , rather than m_\perp . This simple and well-understood dependence leads us to conclude that m_t scaling of the transverse radius cannot be due to hydrodynamic expansion, and it is even doubtful that it is at all possible.

In the case of small differences in radial particle rapidity, the exact result (3.7) may be simplified to obtain the same ‘‘radii’’ for the sideways and outward directions:

$$R_{exp} = \tau \sqrt{\frac{T_c}{m_z}}, \quad R_{cos} = \frac{1}{T_c \tau} R_{exp} , \quad (3.9)$$

where R_{exp} dominates the shape of the correlator for $T_c \tau > 1$, while R_{cos} dominates for $T_c \tau < 1$. If the radial flow takes place against the background of a strong longitudinal expansion, which is likely in a more realistic scenario of the heavy ion collision, the distinctive m_z -dependence in the data could be only washed out, but not replaced by an m_\perp -dependence.

3. Scale-invariant 3-d flow and the explosion of a point-like source: For the case of spherical expansion, $x^\mu = \tau (\cosh \beta, \sinh \beta \sin \theta \cos \psi, \sinh \beta \sin \theta \sin \psi, \sinh \beta \cos \theta)$, with $\tau T_c = \text{const}$, $u^\mu = x^\mu/\tau$, and $d\Sigma^\mu = u^\mu \tau^3 \sinh^2 \beta \sin \theta d\beta d\theta d\psi$. Once again, the emission function $J(k_1, k_2)$ may be evaluated exactly, and we obtain:

$$k^0 \frac{dN_1}{d\vec{k}} = J(k, k) = 4\pi \tau^3 T_c K_2\left(\frac{m}{T_c}\right) , \quad (3.10)$$

$$C_2(k_1, k_2) - 1 = \text{Re} \left[\frac{K_2(H)}{H^2 K_2(m/T_c)} \right]^2 \left[1 + \frac{Q^2}{8m^2} \right]^2 , \quad \text{where } H \equiv \sqrt{1 + T_c^2 \tau^2 \frac{Q^2}{m^2} - i \frac{T_c \tau Q^2}{2m^2}} ,$$

and K_2 is the modified Bessel function. We see that spherically symmetric boost-invariant expansion washes out any inhomogeneity of the local thermal spectrum. This is a distinctive feature of the spherical model. Approximating the correlator in the case of small differences in radial particle rapidity, we obtain

$$C_2(Q) - 1 = e^{-T_c \tau^2 Q_{out}^2/m} \frac{1 + Q^2/4m^2}{1 + 5T_c^2 \tau^2 Q^2/2m^2} \cos \left(\frac{Q^2}{m^2} \left(\frac{5T_c \tau}{2} + \frac{m\tau}{2} \right) \right) . \quad (3.11)$$

All comments related to Eq. (3.9) apply here, too. Here, however, all three directions are physically equivalent and the mass of the particle becomes the only parameter that may re-scale the correlation radius.

IV. CONCLUSION

We have emphasized some important physical aspects of the theory of interferometry, and tried to isolate some controversial points. Strictly speaking, interferometry does not permit the initial data to be given in terms of semi-classical distributions, unless this description is augmented by a clear indication of the length scale that defines the

quantum states of the particles. Our conclusion is that the traditional operator approach, based on the precise definition of the particle states, provides a firm footing for the calculation of the two-particle spectra.

Recent preliminary results by NA35 and NA44 seem to confirm the main predictions of interferometry for a scale-invariant 1-d flow scenario. They provide a multidimensional test of the source, and the fact that so many parameters coincide can hardly be accidental. Thus, we have strong evidence that at SPS energies a hydrodynamic regime develops, and that freeze-out takes place during a short interval. This collective behavior can be expected to occur at RHIC energies, and thus it is highly desirable to continue developing the formalism.

We have extended previous calculations [7] for a longitudinally expanding system to the case of unequal transverse momenta, and have shown that the HBT correlator may carry information about the time of the kaon emission. We further considered transversally expanding sources, and demonstrated how to change the parameterization of the correlator. Unfortunately, the attractive feature that the spectrum is localized in the boost-invariant solution for 1-d flow is absent in 2- and 3-dimensional flows, even if the radial motion is very strong. This happens because the angular dependence of the Cartesian velocity components is weak, and practically means that one should perform all integrations exactly. While even moderate radial flow does obscure the true transverse source size, the spectrum is not sufficiently localized to allow one to obtain a simple formula for the correlator (at least in terms of standard variables). Numerical calculations are, of course, possible, but then it becomes difficult to “recognize” the model.

We emphasize that while HBT for hydrodynamic sources is well understood as a physical phenomenon, choosing an adequate model to fit the data always poses difficulties. We impose the condition that the model should allow one to recognize it via a qualitative analysis. Only then can one hope to understand what parameters are responsible for the behavior of the correlator, and find their values by fitting the data. Practically, this requirement means that we must begin with an analytic expression for a solution of the relativistic hydrodynamic equations. This guarantees the consistency between the shape of the freeze-out surface and the velocity field. Unfortunately, analytic solutions for the case of three-dimensional expansion are not yet known. A reasonable analytic approximation will do, but to our knowledge, a suitable expression has not yet been derived. An approximate formula describing a realistic, expanding system at the freeze-out stage is an important problem for boson interferometry at RHIC.

Acknowledgment: This work was supported in part by the U.S. Department of Energy under Contract No. DE-FG02-94ER40831.

V. REFERENCES

1. Based on: A. Makhlin, E. Surdutovich, and G. Welke, Preprint WSU-NP-94-1 (1994).
2. See, for example: M.I. Podgoretskii, *Sov. J. Part. Nucl.* **20**, 266 (1989).
3. A. Makhlin, *Sov. Phys. JETP* **35**, 478 (1972).
4. S. Pratt, *Phys. Rev. Lett.* **53**, 1219 (1984).³
5. The NA35 collaboration: R. Morse *et al.*, Preprint LBL-36062 (1994).
6. The NA44 collaboration: H. Beker *et al.*, Preprint CERN-PPE/94-119 (1994).
7. A. Makhlin, and Yu. Sinykov, *Sov. J. Nucl. Phys.* **46**, 354 (1987);
V. Averchenkov, A. Makhlin, and Yu. Sinykov, *Sov. J. Nucl. Phys.* **46**, 905 (1987).
8. A. Makhlin, *Sov. J. Nucl. Phys.* **49**, 238 (1989).
9. J. Rafelski, *Phys. Repts.* **331** (1982).

³For an expanding hydrodynamical shell the “visible” source size is smaller the larger the pair’s total momentum. In nuclear collision models, the collision dynamics may result in a more complicated dependence: G. M. Welke, *et al.*, in *Proc. of the 10th Winter Workshop on Nuclear Dynamics*, January 15-22, 1994, Snowbird, Utah (World Scientific, Eds. J. Harris, A. Mingerey, and W. Bauer) p. 93.